This is an electronic reprint of the original article.
This reprint *may differ* from the original in pagination and typographic detail.

Author(s): Kiesilä, Anniina; Kivijärvi, Lauri; Beyeh, Ngong Kodiah; Moilanen, Jani; Groessl, Michael; Rothe, Tatiana; Götz, Sven; Topic, Filip; Rissanen, Kari; Lützen, Arne; Kalenius, Elina

Title: Simultaneous Endo- and Exo-Complex Formation of Pyridine[4]arene Dimer with Neutral and Anionic Guests

Year: 2017

Version:

Accepted Article

This manuscript has been accepted after peer review and appears as an Accepted Article online prior to editing, proofing, and formal publication of the final Version of Record (VoR). This work is currently citable by using the Digital Object Identifier (DOI) given below. The VoR will be published online in Early View as soon as possible and may be different to this Accepted Article as a result of editing. Readers should obtain the VoR from the journal website shown below when it is published to ensure accuracy of information. The authors are responsible for the content of this Accepted Article.

WILEY-VCH

COMMUNICATION

Simultaneous *Endo*- and *Exo*-Complex Formation of Pyridine[4]arene Dimer with Neutral and Anionic Guests

A. Kiesilä,[a] L. Kivijärvi,[a] N.K. Beyeh,[b] J. O. Moilanen,[a] M. Groessl,[c] T. Rothe,[d] S. Götz,[d] F. Topić,[a] K. Rissanen,[a] A. Lützen,[d]* and E. Kalenius[a]*

Abstract: Complex formation between hexafluorophosphate (PF_6^-) and tetraisobutyl-octahydroxypyridine[4]arene (**1**) has been thoroughly studied in gas phase (ESI-QTOF-MS, IM-MS, DFT calculations), solid state (X-ray crystallography) and in chloroform solution (^{1}H, ^{19}F and DOSY NMR). In all states of matter, simultaneous *endo*-complexation of solvent molecules and *exo*-complexation of PF_6^- anion within pyridine[4]arene dimer was observed. While similar ternary complex formation is often observed in solid state, this is a unique example of such behaviour in the gas phase that has never been observed so far.

Resorcinarenes, their derivatives, and their dimeric and hexameric assemblies have found numerous applications in molecular recognition as binding motifs for neutral molecules and cations but also for anions.[1] Over the years, however, there have been contradicting reports on the actual binding site for anionic guests: Dimeric capsules, for example, bind separated ion pairs by encapsulating the cation in the cavity of the dimeric capsule with the anion bound at the lower rim via alkyl- and aryl-CH-anion interactions as evidenced by X-ray diffraction analysis.[2] Likewise, a monomeric cavitand was found to bind ion pairs in a similar fashion in solution, with the anion located at the lower rim between the alkyl chains.[3] Such an arrangement was somewhat counterintuitive, especially regarding our previous work on anion binding with functionalized cavitands in the gas phase where computational studies suggested binding of the anions at the upper rim via CH-anion hydrogen bonding involving the H atoms of the acetal bridges.[4] Nevertheless, this study clearly revealed that anion binding is significantly enhanced by functionalizing the cavitand with electron-withdrawing groups. Therefore, the corresponding pyridine[4]arenes[5] derived from the condensation of 2,6-dihydroxypyridine[6] and aldehydes seemed even more promising for this purpose. They are even more electron deficient and present a unique array of hydrogen bond donor and acceptor functions fixing these molecules in cone conformation. Pioneering work by Mattay already suggested octahydroxypyridine[4]arenes to have affinity towards anions.[7] Rozhenko's theoretical studies

on octahydroxypyridine[4]arene, without lower rim alkyl chains, strongly supported the encapsulation of anionic guests inside the dimer, located in the middle of the cavity close to the hydrogen bonded seam of the dimer. The computational studies showed that anions like tetrafluoroborate and hexafluorophosphate are optimally sized for encapsulation inside the dimer.[8] Moreover, the complexation of carboxylates was experimentally observed, but the mass spectrometric investigation also suggested that the guest could actually be located outside the cavity, with the IRMPD experiments showing the elimination of the guest as the first dissociation step.[7]

Therefore, we decided to thoroughly re-investigate the anion binding behaviour of these interesting but least studied members of the family of resorcinarenes, choosing tetraisobutyl-octahydroxy-pyridine[4]arene (**1**, Scheme 1) to study its binding behavior towards hexafluorophosphate (PF_6^-) in solution (NMR), the solid state (X-ray crystallography), and the gas phase (ESI-MS, IM-MS, DFT calculations) as a first example.
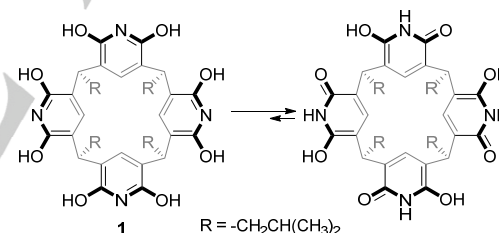
Scheme 1. Tautomerism of tetraisobutyloctahydroxypyridine[4]arene **1** (only one of the two possible enantiomers of the pyridone tautomer is shown).

Cohen earlier showed by ^{1}H DOSY NMR that the tetraundecyloctahydroxypyridine[4]arene forms an equilibrium of dimeric and hexameric aggregates in chloroform solution.[9] The ^{1}H NMR spectra of 10 mM solution of **1** in chloroform clearly show the formation of dimeric capsule-like aggregates, indicated by the signals at 7.10, 4.28 and 1.90 ppm (Figure 1), which can be assigned to the dimeric species by DOSY NMR. These signals give a diffusion coefficient of $0.411 \cdot 10^{-5}$ cm^{2}s^{-1} which is comparable with the $0.37 \cdot 10^{-5}$ cm^{2}s^{-1} value measured for tetraundecyloctahydroxypyridine[4]arene dimer by Cohen.[9]

Interestingly, the ^{1}H NMR spectra measured of equimolar solutions of **1** and TBAPF$_6$ in chloroform (Figure 1) show significant, albeit small downfield shifts for the signals of the Ar-H protons H$_a$ and the CH$_2$ protons H$_c$ at the lower rim of the pyridinearene, in accordance with the observations of Diederich and Dalcanale[3] and resulting from weak CH-anion interactions between the PF_6^- anion and the dimer of **1**. This is a strong

[a] University of Jyväskylä, Department of Chemistry, Nanoscience Center, P.O. Box 35, FI-40014 University of Jyvaskyla, Finland.
E-mail: elina.o.kalenius@jyu.fi
[b] Aalto University, School of Science, Department of Applied Physics, Puumiehenkuja 2, FI-02150 Espoo, Finland
[c] TOFWERK, Uttigenstr. 22, 3600 Thun, Switzerland.
[d] University of Bonn. Kekulé-Institute of Organic Chemistry and Biochemistry, Gerhard-Domagk-Str. 1, D-53121 Bonn, Germany.
E-mail: arne.luetzen@uni-bonn.de

Supporting information for this article is given via a link at the end of the document.

COMMUNICATION

indication that the anion is bound on the exterior of the dimeric capsule, and not inside the cavity as suggested by the previous reports.
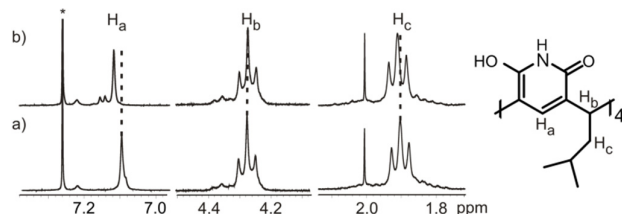

Figure 1. Selected regions of ^{1}H NMR spectra (10 mM, CDCl$_3$, 298 K) of a) **1** and b) **1** + TBAPF$_6$ (1:1). Shift was observed in H$_a$ (0.02 ppm) and smaller shift in H$_c$ (0.01 ppm). CDCl$_3$ marked with an asterisk.

Additional proof for such *exo*-interactions came from the comparison of the ^{19}F NMR spectra of the TBAPF$_6$ and **1**+TBAPF$_6$ samples. Significant downfield shift of the fluorine atoms signals (Figure 2) was observed upon binding of hexafluorophosphate.[10] The fact that only a single set of downfield shifted signals of the guests is observed suggests a fast exchange and/or tumbling motion of the almost spherical anion within its binding pocket on the NMR time scale. While the *endo*-complexation would be expected to result in the shielding of the guests and an upfield shift of the guest signals a downfield shift, however, agrees very well with weak CH-anion interactions, again strongly supporting *exo*-complexation of the anion with **1**.
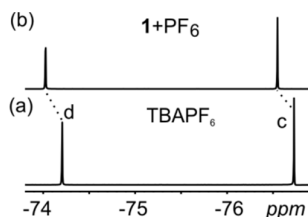

Figure 2. Selected regions of the ^{19}F NMR spectra (20 mM, CDCl$_3$, 298 K) observed from: a) TBAPF$_6$ and b) **1**+TBAPF$_6$ (1:1).

Single crystals of the **1**+TBAPF$_6$ complex were obtained from a chloroform solution of **1** and 3 eq. TBAPF$_6$, by slow evaporation at around 4 °C. The crystal structure (Figure 3) shows **1** in the pyridone tautomeric form (see Table S1). Its cone conformation is stabilized by four intramolecular (hydroxyl)O−H···O(amide) hydrogen bonds with lengths of 2.524(5), 2.553(5), 2.571(6) and 2.609(5) Å, unidirectionally oriented along the upper rim in a clockwise manner. Similarly, the isobutyl groups are aligned unidirectionally along the lower rim with the methane CH groups in an anticlockwise arrangement. Next, two molecules of **1** form a dimeric capsule sustained by eight N−H···O(amide) hydrogen bonds, with the lengths of symmetrically independent hydrogen bonds of 2.822(6), 2.872(6), 3.108(6) and 3.115(8) Å. The latter two hydrogen bonds are elongated due to bifurcation, as both the NH donors and O(amide) acceptors are also engaged in hydrogen

bonding with the neighbouring capsule (3.018(6) and 3.040(5) Å long, Figure S1 in SI). Instead of PF$_6^-$ anion, we found the dimer cavity fully occupied by a CHCl$_3$ molecule.[11] On the other hand, the PF$_6^-$ anion was found to reside on the lower rim of **1**, in a slightly asymmetric tilted orientation within the pocket formed by the four isobutyl groups. To the best of our knowledge this is the first solid state structure of a pyridinearene host-guest complex and such a motif of simultaneous *endo*-binding of a solvent molecule and *exo*-binding of an anion has never been observed for any other resorcinarene system. The apical fluorine atom of PF$_6^-$ forms short contacts with the four lower rim aromatic CH protons, with respective C−H···F hydrogen bond lengths of 3.445(8), 3.516(8), 3.566(7) and 3.616(7) Å, as well as with the isobutyl groups. Equatorial fluorine atoms further form a number of C−H···F hydrogen bonds with the isobutyl groups. The PF$_6^-$ anion is further surrounded by two CHCl$_3$ molecules and the tetrabutyl ammonium (TBA$^+$) cation, also forming a number of C−H···F hydrogen bonds (Figure S2 in SI).
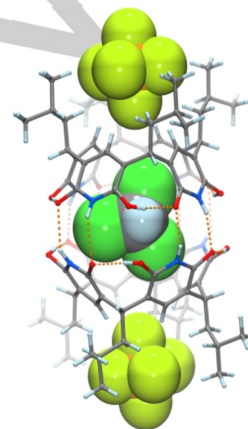

Figure 3. Crystal structure of $[\mathbf{1}_2 + 2PF_{6(exo)} + CHCl_{3(endo)}]^{2-}$. *Endo*-complexed CHCl$_3$ and *exo*-complexed PF$_6^-$ are shown in space-filling model. Hydrogen bonds are shown as dashed orange lines. TBA$^+$ cations and co-crystallized CHCl$_3$ solvent molecules are omitted for clarity.

The spontaneous self-assembly of **1** into dimeric ions was also clearly observed in ESI-MS spectra. In addition to the deprotonated ion $[\mathbf{1}_2−H]^-$ at *m/z* 1432 and anion complex $[\mathbf{1}_2+PF_6]^-$ at *m/z* 1578, abundant formation of solvent adduct $[\mathbf{1}_2−H+S]^-$ (S = solvent, e.g. acetone, acetonitrile or CH$_2$Cl$_2$, depending on sample solvent) and ternary complex $[\mathbf{1}_2+PF_6+S]^-$ were clearly detected (Figure 4).[10] Even though the formation of solvent adducts or even inclusion of solvent molecules is relatively common in condensed phase where the solvent often fills the void space, this phenomenon is extremely surprising and novel in gas phase and has – to the best of our knowledge – never been described in any anion- or cation-binding study with resorcinarenes before. It is important to note that the monomer region of the mass spectra did not show any peaks corresponding to solvent adducts such as $[\mathbf{1}-H+S]^-$ or $[\mathbf{1}+PF_6+S]^-$, implying that the phenomenon is indeed a feature of the dimer via inclusion, and not adduct formation.
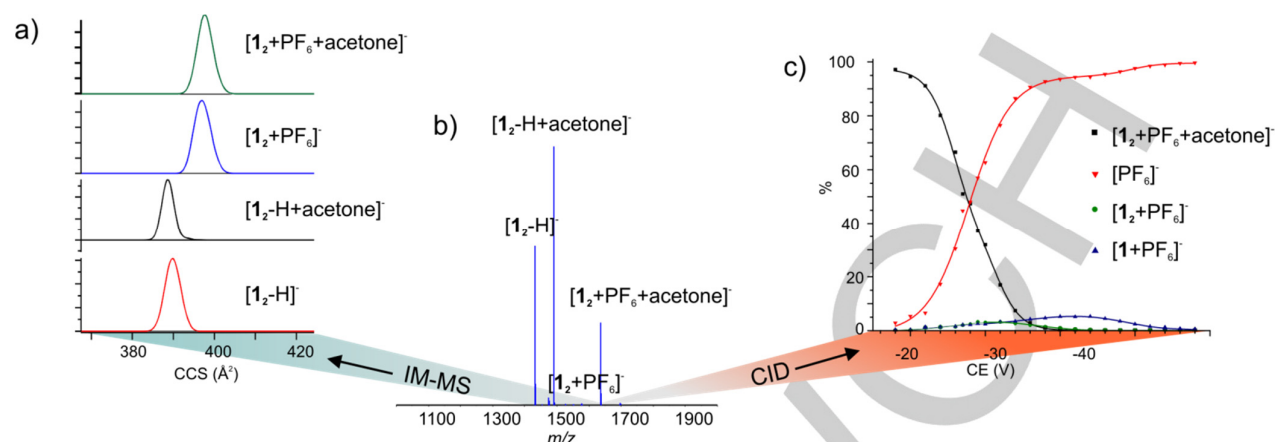
COMMUNICATION

Figure 4. a) IM-MS ion mobilograms for selected ions, b) ESI-MS spectrum of **1** with equimolar ratio of NH_4PF_6 in acetone and c) CID dissociation curve for isolated ion [1_2+PF$_6$+acetone]$^-$.

When ternary complex, [1_2+PF$_6$+acetone]$^-$, was isolated in gas phase and activated in collision-induced dissociation (CID) experiment, PF$_6^-$ anion was eliminated in the initial dissociation step. CID is an ergodic activation technique and due to energy randomization the weakest bond or interaction is generally broken first. Elimination of the anion as the initial dissociation step, implies to weak and *exo*-complexation of PF$_6^-$ with pyridinearene **1**, since only small amounts of other dissociation products were observed. In the case of *endo*-complexed PF$_6^-$ and *exo*-complexed solvent, elimination of solvent or pyridinearene monomer would be expected as the first step. Definitive proof for the *exo*-complexation of anion in the gas phase was obtained by drift tube ion-mobility mass spectrometry (DTIM-MS) experiments.[12,13] IM-MS is still rarely utilized tool in supramolecular chemistry despite its benefits in the detection of host-guest complexes and the analysis of conformers and structural features.[14] As the drift tube of the IM-MS instrument is operated at atmospheric pressure, it allows high resolution separations and therefore accurate determination of collision cross section (CCS) values[15] without the need for cumbersome calibration, which often severely complicates the analysis when the more common TW-IM-MS (travelling-wave ion-mobility MS) is used. The ion mobilograms (Figure 4a) show very similar but clearly larger ^{DT}CCS$_{N2}$ values for ions [1_2+PF$_6$+acetone]$^-$ and [1_2+PF$_6$]$^-$ compared to ions [1_2−H]$^-$ and [1_2−H+acetone]$^-$. In terms of collision cross sections (CCS), the PF$_6^-$ complexes are ~8 Å^2 larger compared to the deprotonated dimer (Table 1).

Therefore, it is reasonable to conclude that, also in the gas phase, the dimers of **1** contain *endo*-complexed solvent and *exo*-complexed anion and can thus be denoted as [1_2+PF$_{6(exo)}$+acetone$_{(endo)}$]$^-$. Assuming the spherical shape for dimer of **1**, the obtained CCS values can be roughly compared with the hydrodynamic radii from the ^{1}H DOSY NMR and the crystal structure (Table 1). Each of the methods results in very similar diameters (1.9 to 2.3 nm), demonstrating structural similarity of dimers in solid state, gas phase, and solution and also highlighting the potential of IM-MS technique for structural chemistry purposes of host-guest systems.

To further analyse the gas phase structures of the observed ternary complexes, we performed density functional theory (DFT) calculations for the dimer and its inclusion complexes *in vacuo* at the RI-PBEPBE/def2-TZVP and RI-PBEPBE/def2-TZVP-D3 levels of theory.[16-18] As mentioned above, previous computational studies suggested the encapsulation of PF$_6^-$ within the octahydroxypyridine[4]arene capsule.[8] However, the lower rim alkyl chains were truncated and the solvent molecules were not modelled explicitly in this earlier study, with the solvent effects included using the COSMO-model only. Therefore, both the *endo*- and *exo*-complexes of PF$_6^-$ with and without acetone were re-examined by simulating the complete structures.

Optimized structures of the inclusion complexes are in good agreement with solid state structures, with the *exo*-complexed PF$_6^-$ showing several F···H interactions with the lower rim alkyl chains of **1**, in [1+PF$_{6(exo)}$]$^-$, [1_2+PF$_{6(exo)}$]$^-$, and [1_2+PF$_{6(exo)}$+acetone$_{(endo)}$]$^-$ (Table S3 and Figure S4).

The calculated interaction energies, given in Table 2, reveal that the *exo*-complexation of PF$_6^-$ is favoured over the *endo*-complexation in all studied systems, except in [1_2+PF$_6$]$^-$, when the dispersion correction is applied. The dispersion-corrected calculation predicts the interaction energy for [1_2+PF$_{6(endo)}$]$^-$ to be ~10 kJmol^{-1} more favourable compared to the one for [1_2+PF$_{6(exo)}$]$^-$. However, this is reversed in case of the ternary complexes, where the [1_2+PF$_{6(exo)}$+acetone$_{(endo)}$]$^-$ is significantly more favoured (by >20 kJmol^{-1}) compared to [1_2+PF$_{6(endo)}$+acetone$_{(exo)}$]$^-$. Interestingly, the dispersion-corrected

Table 1. Experimental ^{DT}CCS$_{N2}$ values and comparison of approximated diameters (nm) obtained by IM-MS, ^{1}H DOSY NMR and X-ray diffraction.

Ion	*m/z*	^{DT}CCS$_{N2}$ (Å^2)	IM-MS[a] *d* (nm)	DOSY *d* (nm)	X-ray *d* (nm)
[1−H]$^-$	715	264.5			
[1_2−H]$^-$	1432	389.8	2.2		
[1_2+acetone−H]$^-$	1490	388.6	2.2		
[1_2+PF$_6$]$^-$	1578	396.9	2.3	2.0[b]	1.9[b]
[1_2+PF$_6$+acetone]$^-$	1636	397.6	2.3		

[a] Diameters calculated on basis of CCS by assuming a spherical conformation.
[b] Diameters for ^{1}H DOSY NMR and X-ray diffraction apply generally to dimers.

COMMUNICATION

interaction energies are much higher (40-120 kJmol^{-1}) than the non-corrected energies underlining the important role of dispersion forces in the formation of the inclusion complexes at hand.

Table 2. Calculated interaction energies for **1** and complexes at the RI-PBEPBE/def2-TZVP (E_{int}) and RI-PBEPBE/def2-TZVP-D3 (E_{int-D3}) levels of theory.

Compound	ΔE_{int} (kJ mol^{-1})	ΔE_{int-D3} (kJ mol^{-1})
[**1**+PF$_{6(exo)}$]$^{-}$ [a]	−122.49	−161.27
[**1**+PF$_{6(endo)}$]$^{-}$ [a]	−56.84	−100.59
[**1**$_2$+PF$_{6(exo)}$]$^{-}$ [b]	−116.90	−155.55
[**1**$_2$+PF$_{6(endo)}$]$^{-}$ [b]	−85.85	−165.88
[**1**$_2$+PF$_{6(exo)}$+acetone$_{(endo)}$]$^{-}$ [c]	−117.03	−239.3
[**1**$_2$+PF$_{6(endo)}$+acetone$_{(exo)}$]$^{-}$ [c]	−105.70	−217.56

[a] $\Delta E_{int} = E_{complex} − (E_{PF6} + E_1)$, [b] $\Delta E_{int} = E_{complex} − (E_{PF6} + E_1)$, [c] $\Delta E_{int} = E_{complex} − (E_{PF6} + E_1 + E_{acetone})$

To visualize the reason for the *exo*-complexation of PF$_6^-$ we mapped the electrostatic potential (ESP) surfaces of the **1**$_2$ dimer and its complexes with acetone and/or PF$_6^-$ (Figure 5). The cavity of the dimer itself does not show any significant positive partial potential. Instead, the seam of hydrogen bonds is clearly polarized and contains electron-rich surfaces implying poor affinity of the cavity towards anions. In contrast to the cavity, however, the lower rim alkyl chains show an electron-poor area that is more suitable for anion binding. The computational data not only supports the experimental finding that the *exo*-complexation of PF$_6^-$ is more favourable than the *endo*-complexation but it also indicates that the guest encapsulation is largely governed by dispersion forces, making the solvent molecules better guests for the *endo*-complexation.
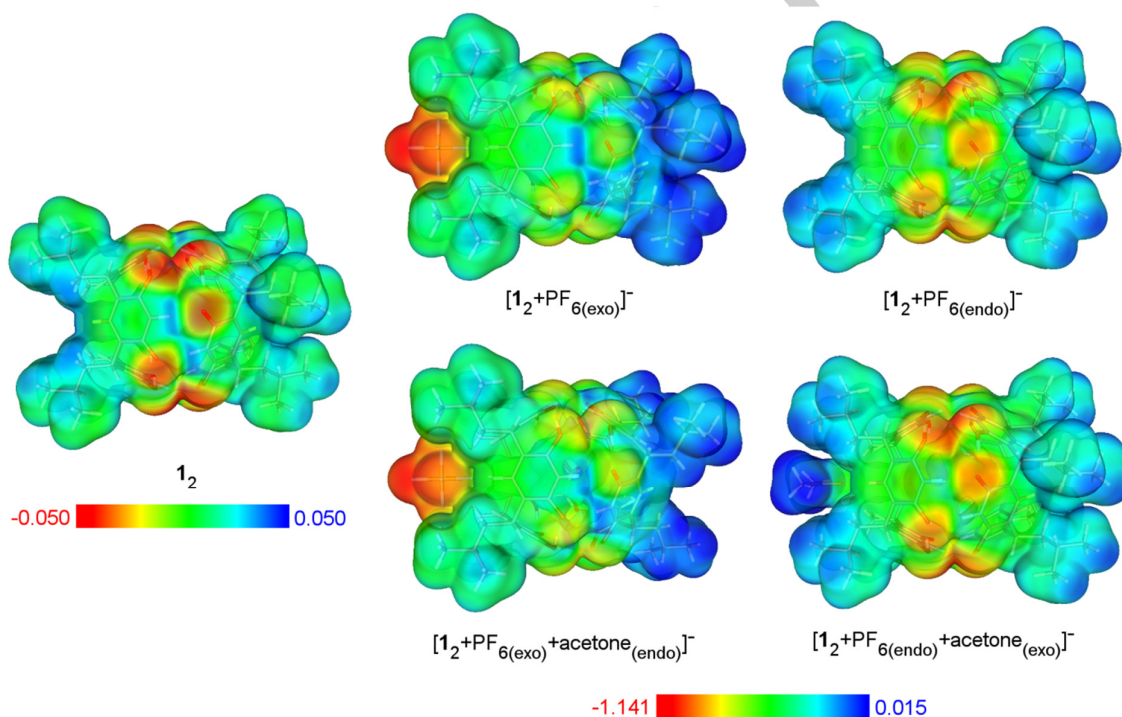

Figure 5. Calculated RI-PBEPBE/def2-TZVP electrostatic potentials for pyridinearene dimer (−0.050 − 0.050 au) and for complexes with PF$_6^-$ and acetone (−1.414 − (−0.015) au) mapped on the isosurface of the total electron density (0.003 au). Top row: [**1**$_2$], [**1**$_2$+PF$_{6(exo)}$]$^{-}$, [**1**$_2$+PF$_{6(endo)}$]$^{-}$, bottom row: [**1**$_2$+PF$_{6(exo)}$+acetone$_{endo}$]$^{-}$, [**1**$_2$+PF$_{6(endo)}$+acetone$_{exo}$]$^{-}$.

In conclusion, we have unambiguously shown the anion complexation by an *exo*-binding site of pyridine[4]arene **1** through CH-anion interactions in gas phase, solid state, and in solution. This is rationalized by the computed electrostatic potential surfaces which, in contradiction to previous reports, show partial positive potential located between the lower rim alkyl chains, not in cavity. In contrast to earlier assumptions, it is clear that the pyridine[4]arene cavity is not particularly well suited to anion binding. Instead, efficient *endo*-complexation of neutral molecules by dispersion interactions and formation of ternary complexes is

detected. Even though the anion binding (*exo*-)site is similar in pyridine[4]arenes and classical resorcinarenes, the binding mode in pyridine[4]arene dimer deviates from that of the latter and is unpresented. Whereas resorcinarenes complex separated ion pairs (cations in cavity and anions at lower rim), the pyridine[4]arene complexes neutral molecules within the cavity and anion on lower rim. Although common in the solid state, similar ternary complex formation has not been previously observed in any gas phase studies of resorcinarenes. This study also shows the importance of utilising novel techniques and

COMMUNICATION

approaches, such as IM-MS to study the structural chemistry of host-guest complexes in gas phase. Preliminary results,[10,11] concerning binding of other anions in variety of other solvents indicate that this binding motif is a unique feature of the pyridinearenes but it is not limited to the combination of the PF_6^- anion and chloroform or acetone but is more general in terms of both the anion, the solvent and the pyridinearene lower rim alkyl chains. We are currently investigating the potential of pyridinearenes in host-guest chemistry in more detail and these results will reported in due course.

Experimental Section

Experimental details for synthesis, NMR, mass spectrometry, DFT calculations and X-ray crystallography are presented in supporting material.

Acknowledgements

Keywords: pyridinearenes • resorcinarenes • molecular recognition • anion binding • ion mobility mass spectrometry

[1] a) H.-J. Schneider, U. Schneider, *J. Incl. Phenom. Mol. Recogn. Chem.* **1994**, *19*, 67-83; b) P. Timmerman, W. Verboom, D. N. Reinhoudt, *Tetrahedron*, **1996**, *52*, 2663-2704; L. C. Palmer, J. Rebek, Jr., *Org. Biomol. Chem*. **2004**, *2*, 3051-3059; d) S. M. Biros, J. Rebek, Jr., *Chem. Soc. Rev*. **2009**, *36*, 93-104; e) N. Li, R. G. Harrison, J. D. Lamb, *J. Incl. Phen. Macrocycl. Chem.* **2014**, *78*, 39-60; f) K. Kobayashi, M. Yamanaka, *Chem. Soc. Rev.* **2015**, *44*, 449-466.

[2] a) A. Shivanyuk, K. Rissanen, E. Kolehmainen, *Chem. Commun.* **2000**, 1107-1108; b) H. Mansikkamäki, M. Nissinen, K. Rissanen, *Chem. Commun*. **2002**, 1902-1903; c) H. Mansikkamäki, M. Nissinen, C. A. Schalley, K. Rissanen, *New J. Chem*. **2003**, *27*, 88-97; d) E. Biavardi, M. Favazza, A. Motta, I. L. Fragalà, C. Massera, L. Prodi, M. Montalti, M. Melegari, G. G. Condorelli, E. Dalcanale, *J. Am. Chem. Soc.* **2009**, *131*, 7447-7455.

[3] F. Tancini, T. Gottschalk, W. B. Schweizer, F. Diederich, E. Dalcanale, *Chem. Eur. J.* **2010**, *16*, 7813-7819.

[4] S. S. Zhu, H. Staats, K. Brandhorst, J. Grunenberg, F. Gruppi, E. Dalcanale, A.Lützen, K. Rissanen, C. A. Schalley, *Angew. Chem.* **2008**, *120*, 800-804; *Angew. Chem. Int. Ed.* **2008**, *47*, 788-792.

[5] T. Gerkensmeier, J. Mattay, C. Näther, *Chem. Eur. J*. **2001**, *7*, 465-474.

[6] Please note, that it is actually more efficient to use 2,6-dimethoxypyridine instead of 2,6-dihydroxypyridine for the synthesis of pyridine[4]arenes. For more details see SI.

[7] M. C. Letzel, B. Decker, A. B. Rozhenko, W. W. Schoeller, J. Mattay, *J. Am. Chem. Soc.* **2004**, *126*, 9669-9674.

[8] A. B. Rozhenko, W. W. Schoeller, M. C. Letzel, B. Decker, J. Mattay, *New J. Chem.* **2013**, *37*, 356-365.

[9] T. Evan-Salem, Y. Cohen, *Chem. Eur. J.* **2007**, *13*, 7659-7663.

[10] Preliminary studies show that a similar *exo*-binding is also found with other anions like BF_4^- and I^- as revealed by NMR and mass spectrometry.

[11] Preliminary studies show that a similar encapsulation of solvent molecules is also found with other solvents like THF and CH_2Cl_2 as revealed by XRD-analysis and mass spectrometry.

[12] F. Lanucara, S. W. Holma, C. J. Gray, C. E. Eyers, *Nat. Chem.* **2014**, *6*, 281-294.

[13] C. Lapthorn, F. Pullen, B. Z. Chowbury, *Mass Spec. Rev.* **2013**, *32*, 43-71.

[14] a) T.-C. Lee, E. Kalenius, A. I. Lazar, K. I. Assaf, N. Kuhnert, C.H. Grün, J. Jänis, O.A. Scherman, W.M. Nau, *Nat. Chem.,* **2013**, *5*, 376-382; b) P. Bonakdarzadeh, F. Topic, E. Kalenius, S. Bhowmik, S. Groessl, R. Knochenmuss, S. Sato and K. Rissanen, *Inorg. Chem.* **2015**, *54*, 6055−6061; c) O. Jurček, P. Bonakdarzadeh, E. Kalenius, J. M. Linnanto, M. Groessl, R. Knochenmuss, R. Puttreddy, J. Ihalainen, K. Rissanen, *Angew. Chem.* **2015**, *54*, 15462-15467; d) E. S. Baker, J. E. Bushnell, S. R. Wecksler, M. D. Lim, M. J. Manard, N. F. Depuis, P. C. Ford, M. T. Bowers, *J. Am. Chem. Soc.* **2005**, *127*, 18222-18228; e) X. Li, Y.-T. Chan, M. Casiano-Maldano, J. Yu, G. A. Carri, G. R. Newkome, C. Wesdemiotis, *Anal. Chem.* **2011**, *83*, 6667-6674; f) J. Ujma, M. De Cecco, O. Chepelin, H. Levene, C. Moffat, S. J. Pike. P. J. Lusby, P. E. Barran, *Chem. Commun.* **2012**, *48*, 4423-4425; g) P. J. Robbins, A. J. Surman, J. Thiel, D.-L. Long, L. Cronin, *Chem. Commun.* **2013**, *49*, 1909-1911.

[15] J. C. May, C. B. Morris, J. A. McLean, *Anal. Chem.* **2017**, *89,* 1032−1044.

[16] (a) P.A.M. Dirac, Proc. Royal Soc. A, **1929**, *123*, 714-733 (b) J.C. Slater, *Phys. Rev.* **1951**, *81*, 385-390. (c) J.P. Perdew, Y. Wang, *Phys. Rev. B*, **1992**, *45*, 13244-13249. (d) J.P. Perdew, K. Burke, M. Ernzerhof, *Phys. Rev. Lett*. **1996**, *77*, 3865-3868

[17] (a) K. Eichkorn, O. Treutler, H. Öhm, M. Häser, R. Ahlrichs, *Chem. Phys. Lett.* **1995**, *242*, 652–660 (erratum, **1995**, *242*, 283-290). (b) K. Eichkorn, F. Weigend, O. Treutler, R. Ahlrichs, *Theor. Chem. Acc.* **1997**, *97*, 119-124.

[18] S. Grimme, J. Antony, S. Ehrlich, H. Krieg, *J. Chem. Phys.* **2010**, *132*, 154104-154104.